Supplementary TABLE 1.

Luciferase mRNA in cytoplasm

The average percentages of NFAT-pGL3 or NFκB-pTransLucent luciferase mRNA in cytoplasm of transduced K562 cells from 3 independent experiments are shown ± standard deviations. The *P* value was obtained by comparing to control using a two-tailed distribution t-test.

	NFAT-pGL3 Luciferase		**NFκB-pTransLucent Luciferase**	
	mRNA in Cytoplasm (%)	*P* value	mRNA in Cytoplasm (%)	*P* value
Control	87.49 ± 1.72		90.99 ± 1.68	
NUP98-HOXA9	88.04 ± 1.83	0.727	89.29 ± 1.17	0.223
NUP98-DDX10	86.75 ± 4.18	0.791	88.48 ± 1.41	0.118

Supplementary Experimental Procedures

Quantitation of luciferase mRNA — K562 cells were transfected by electroporation as described for *Luciferase reporter assays* in Experimental Procedures but without pRL-TK. Cytoplasmic and nuclear RNA was prepared from each transfected sample after 48 h culture using Cytoplasmic & Nuclear RNA Purification kit and RNase-free DNase I kit (Norgen Biotek Corp., Thorold, Canada). For quantitation of NFAT-pGL3 and NFκB-pTransLucent mRNA by quantitative PCR (qPCR), template cDNA was synthesized using SuperScript III First-strand Synthesis System for RT-PCR (Invitrogen). qPCR was carried out using B-R SYBR Green Supermix (Quanta Biosciences Inc., Gaithersburg, MD) in StepOnePlus Real-Time PCR System (Applied Biosystems, Foster City, CA) with the following primer sets: 5'-AAGAAGGGCGGAAAGATCG-3' with oligo$(dT)_{30}$ for NFAT-pGL3; 5'-TTACCGGAAAACTCGACGC-3' with oligo$(dT)_{30}$ for NFκB-pTransLucent. The amount of transcript in the cytoplasm and nucleus was determined based on a standard curve specific for each luciferase and normalized to the amount of glyceraldehydes phosphate dehydrogenase transcript, and the percentage of luciferase mRNA in cytoplasm was calculated.

A

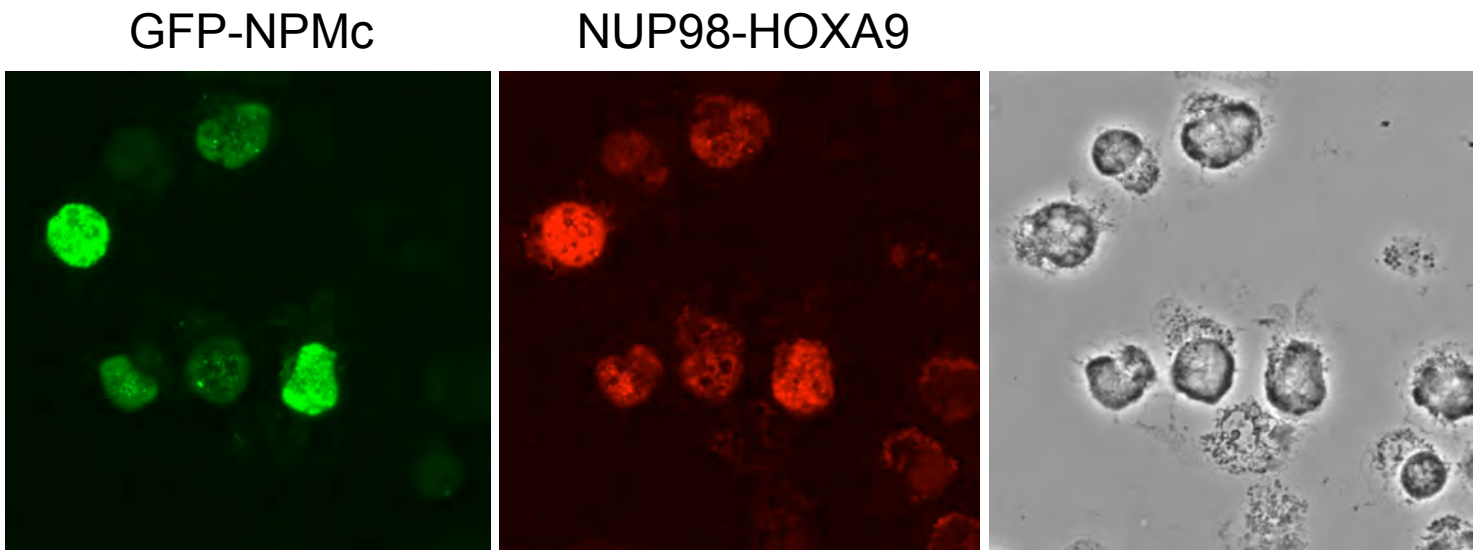

B

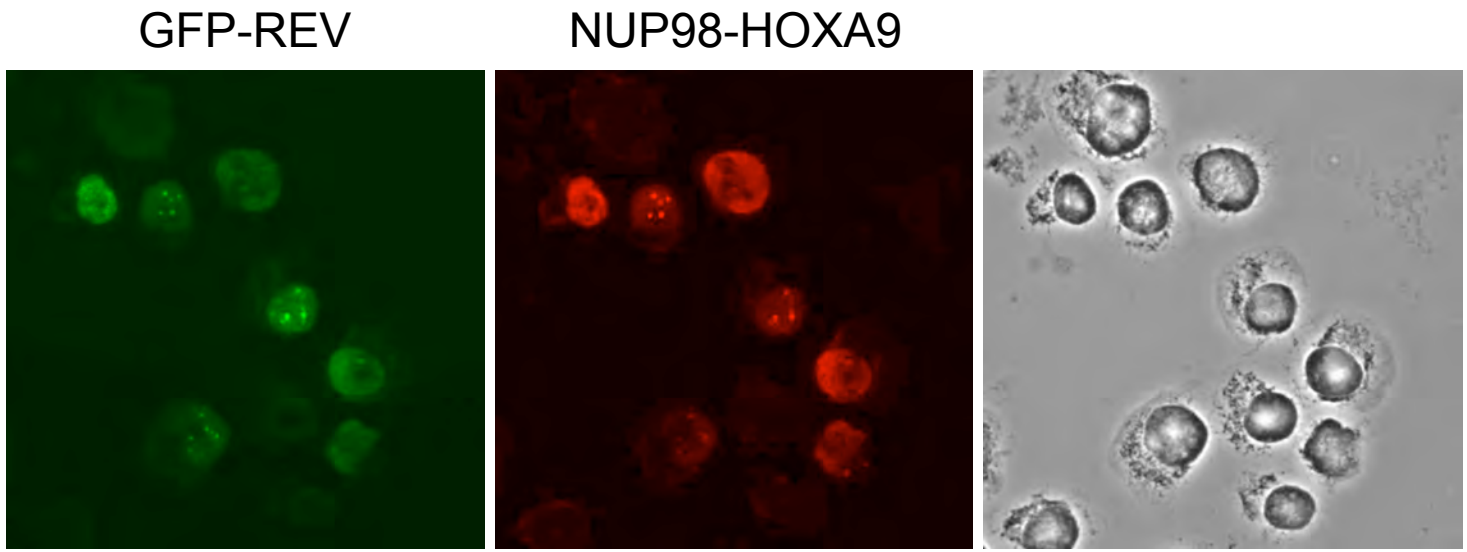

Supplementary Fig. 1

A

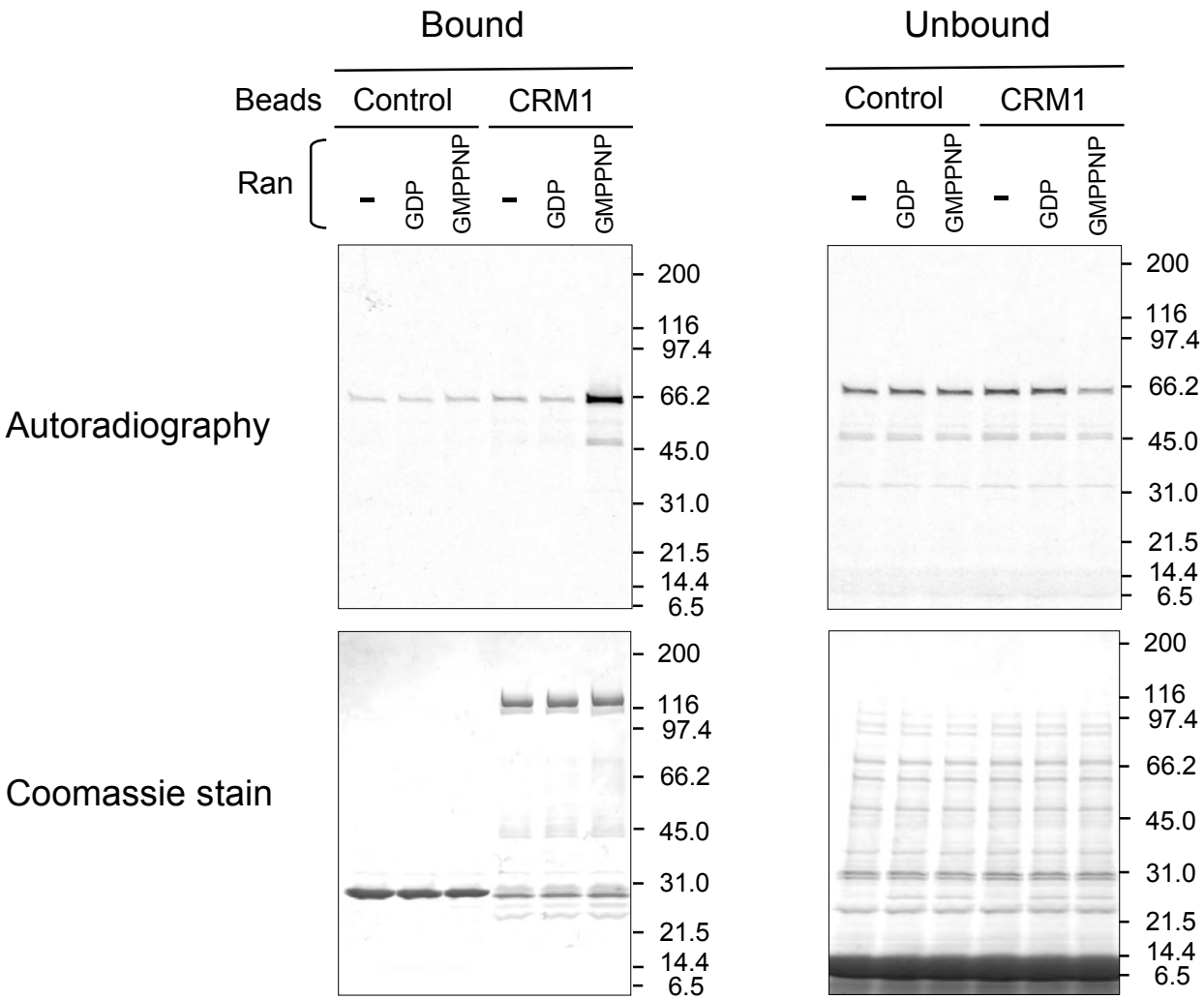

Supplementary Fig. 2A

B

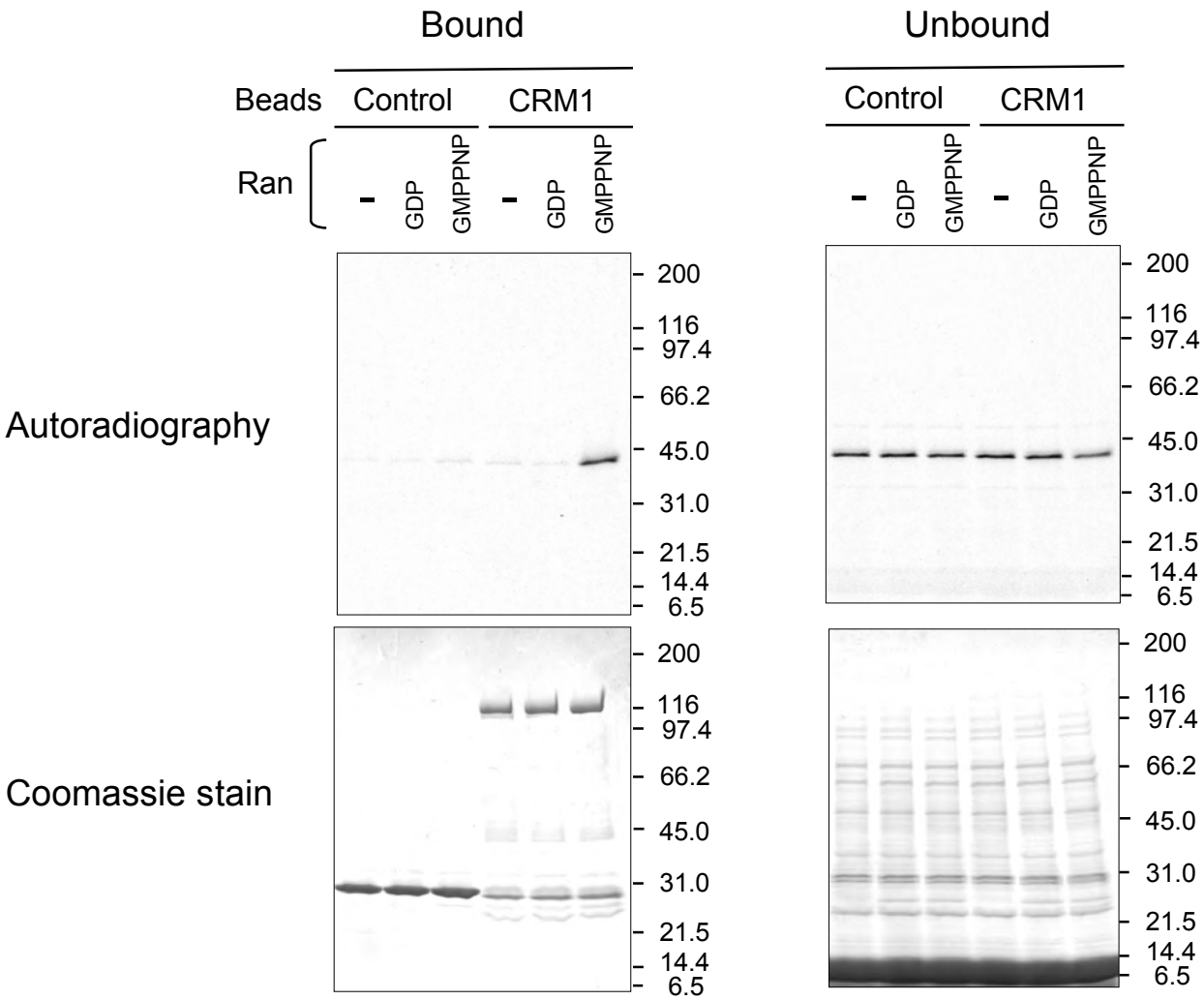

Supplementary Fig. 2B

C

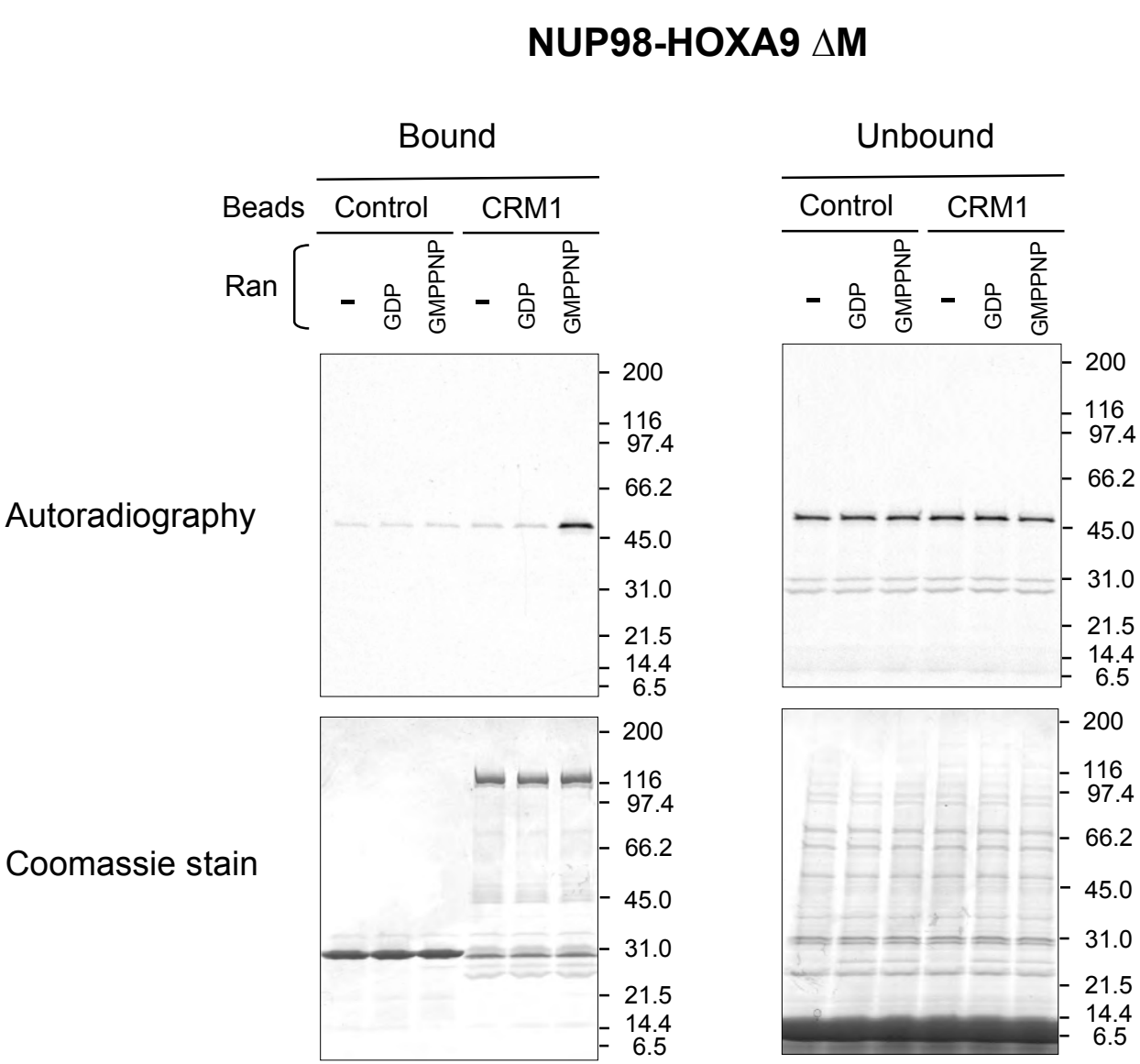

Supplementary Fig. 2C

D

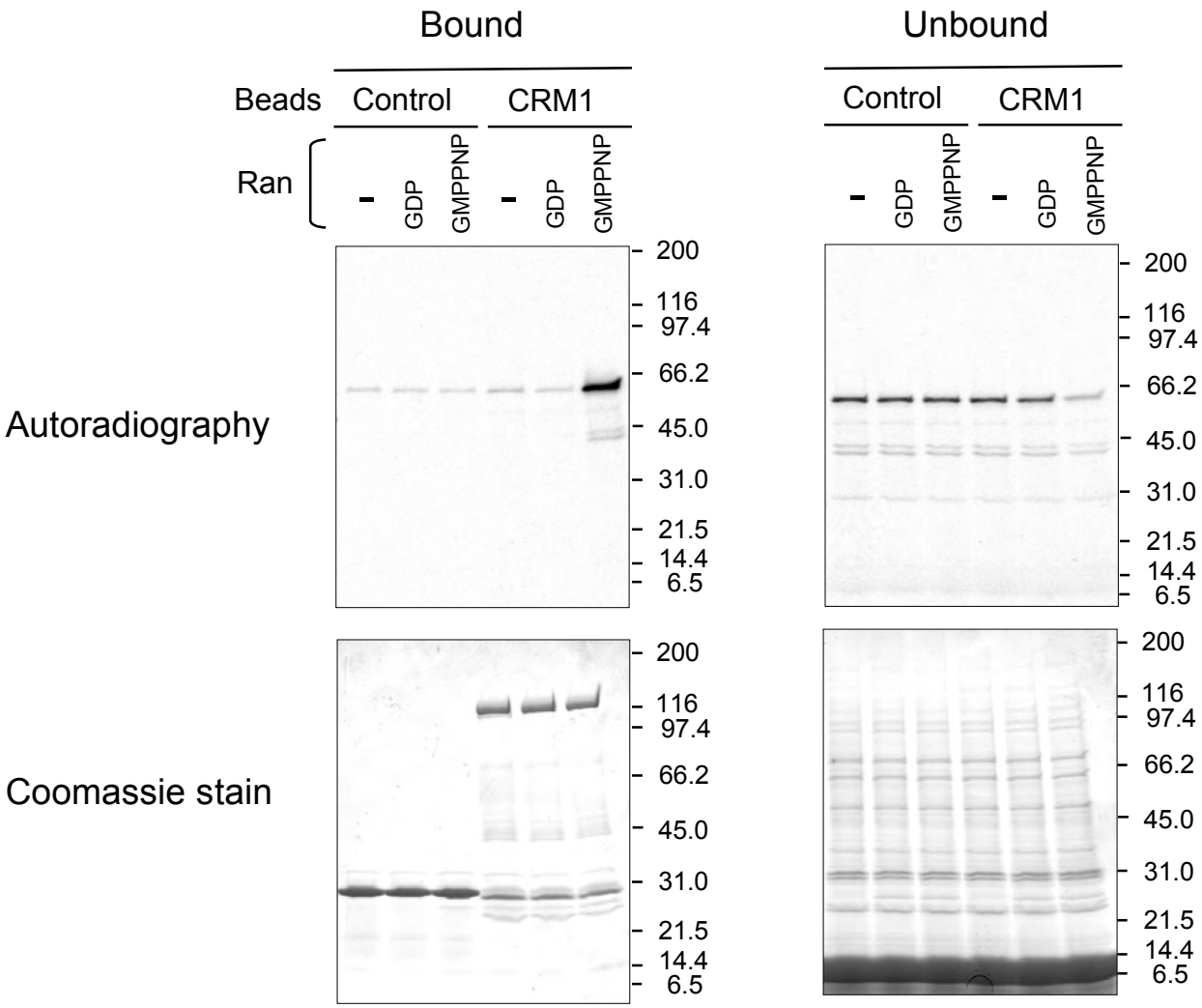

Supplementary Fig. 2D

E

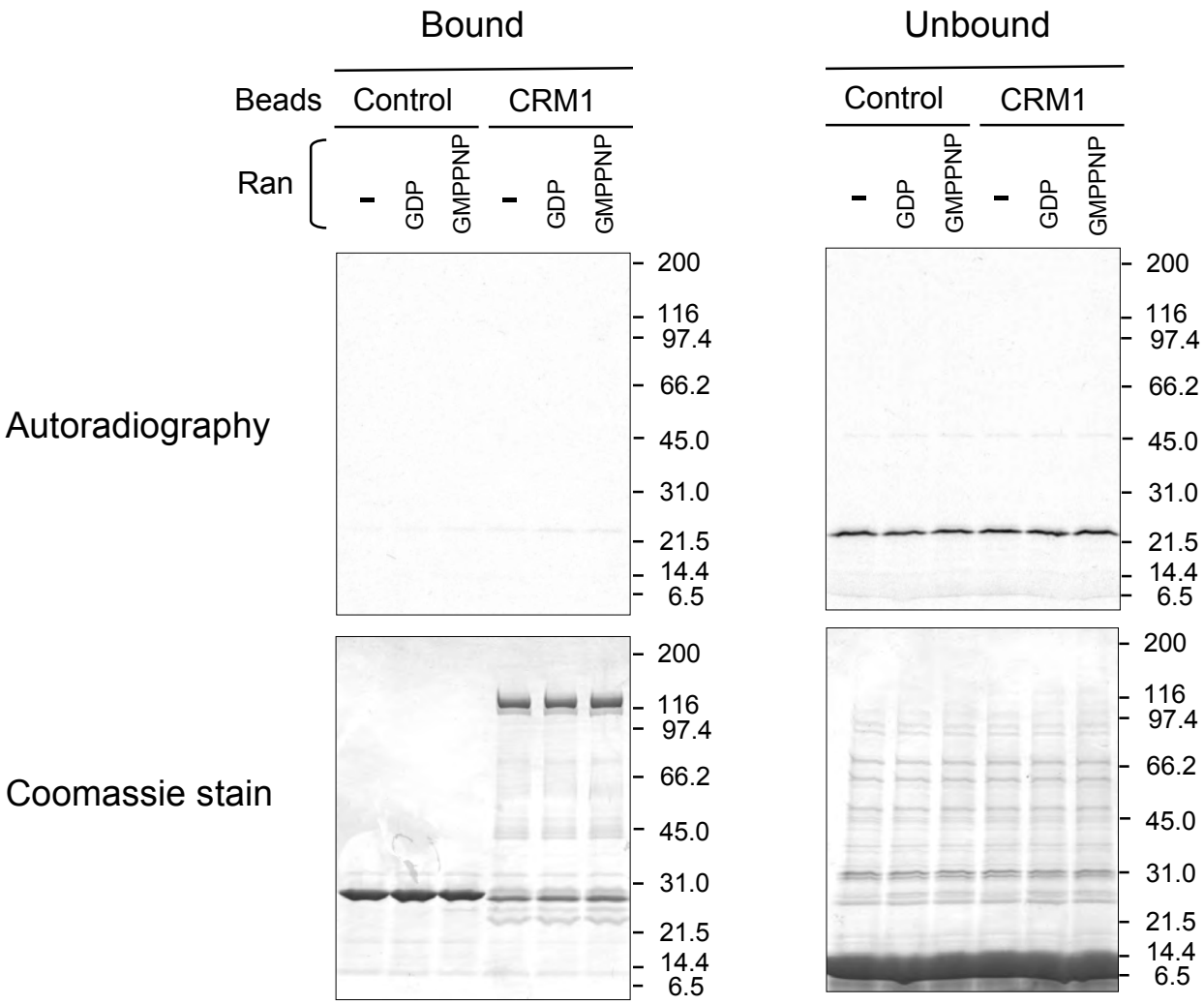

Supplementary Fig. 2E

F

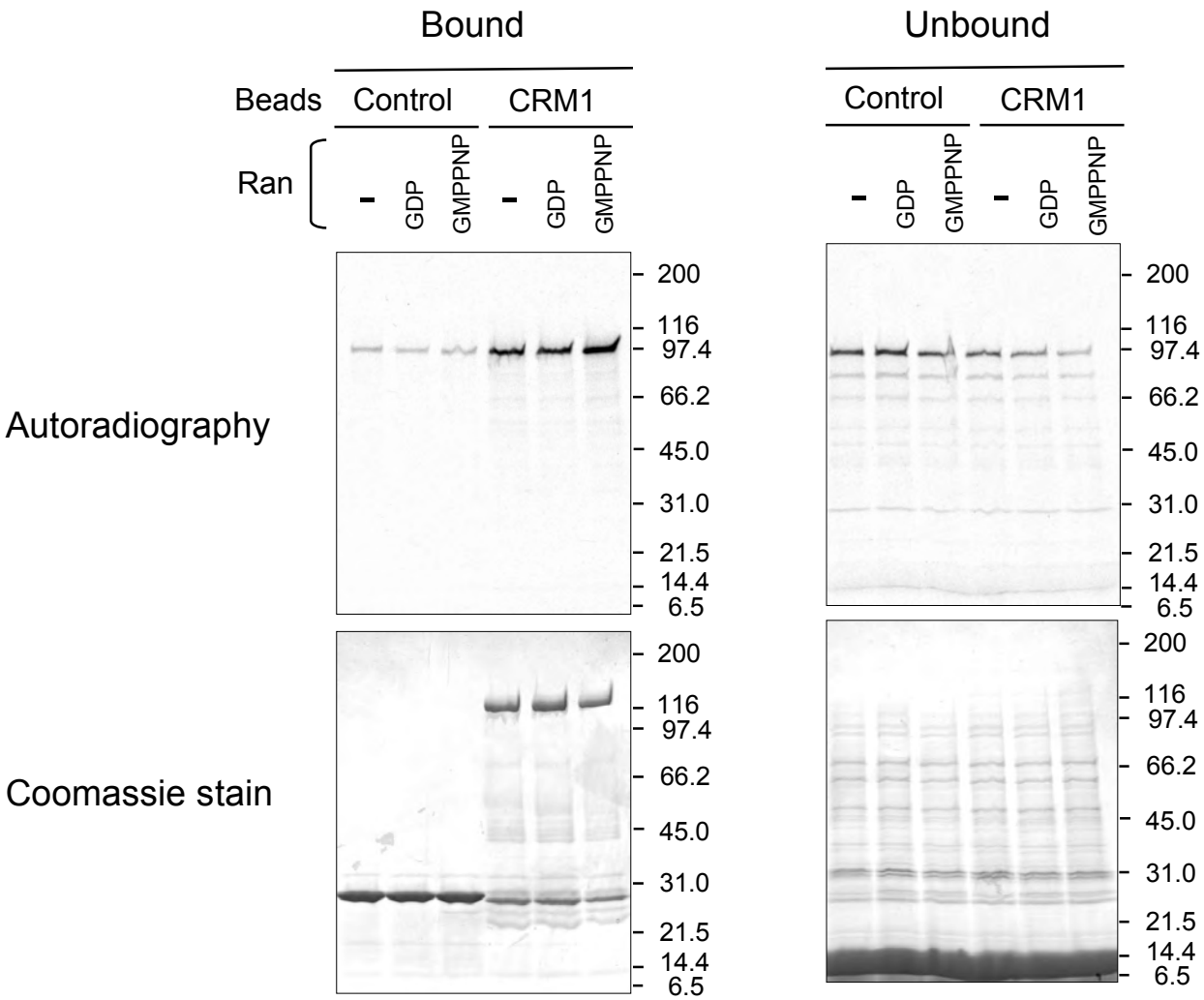

Supplementary Fig. 2F

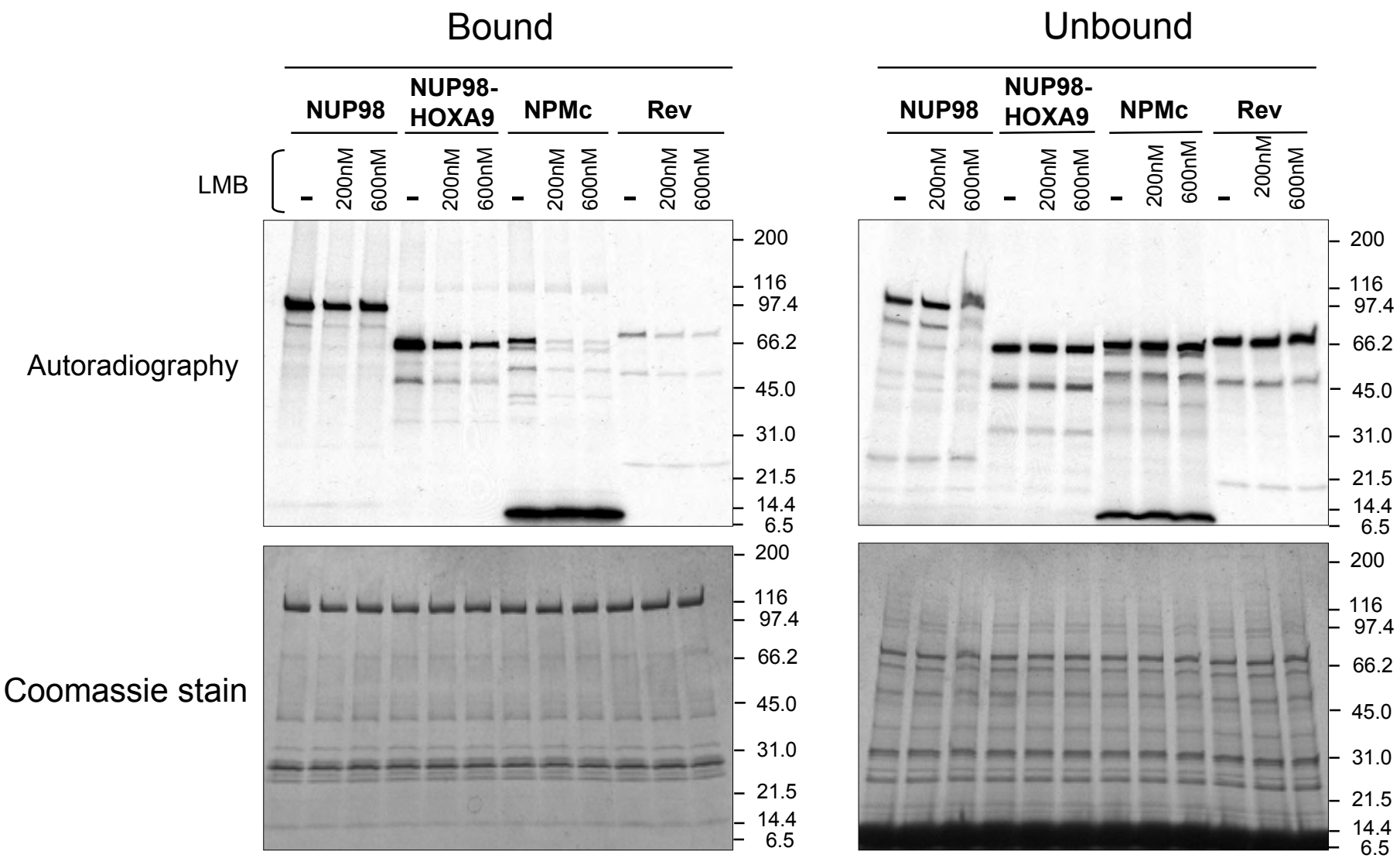

Supplementary Fig. 3

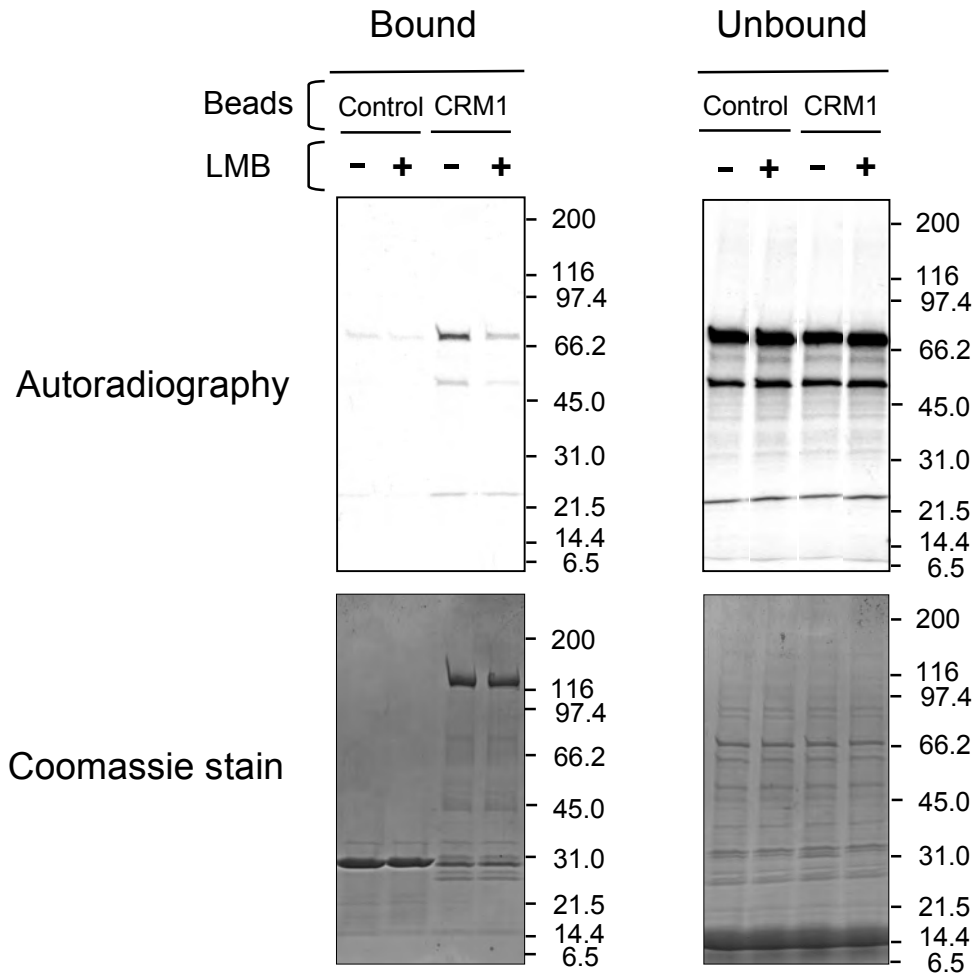

Supplementary Fig. 4

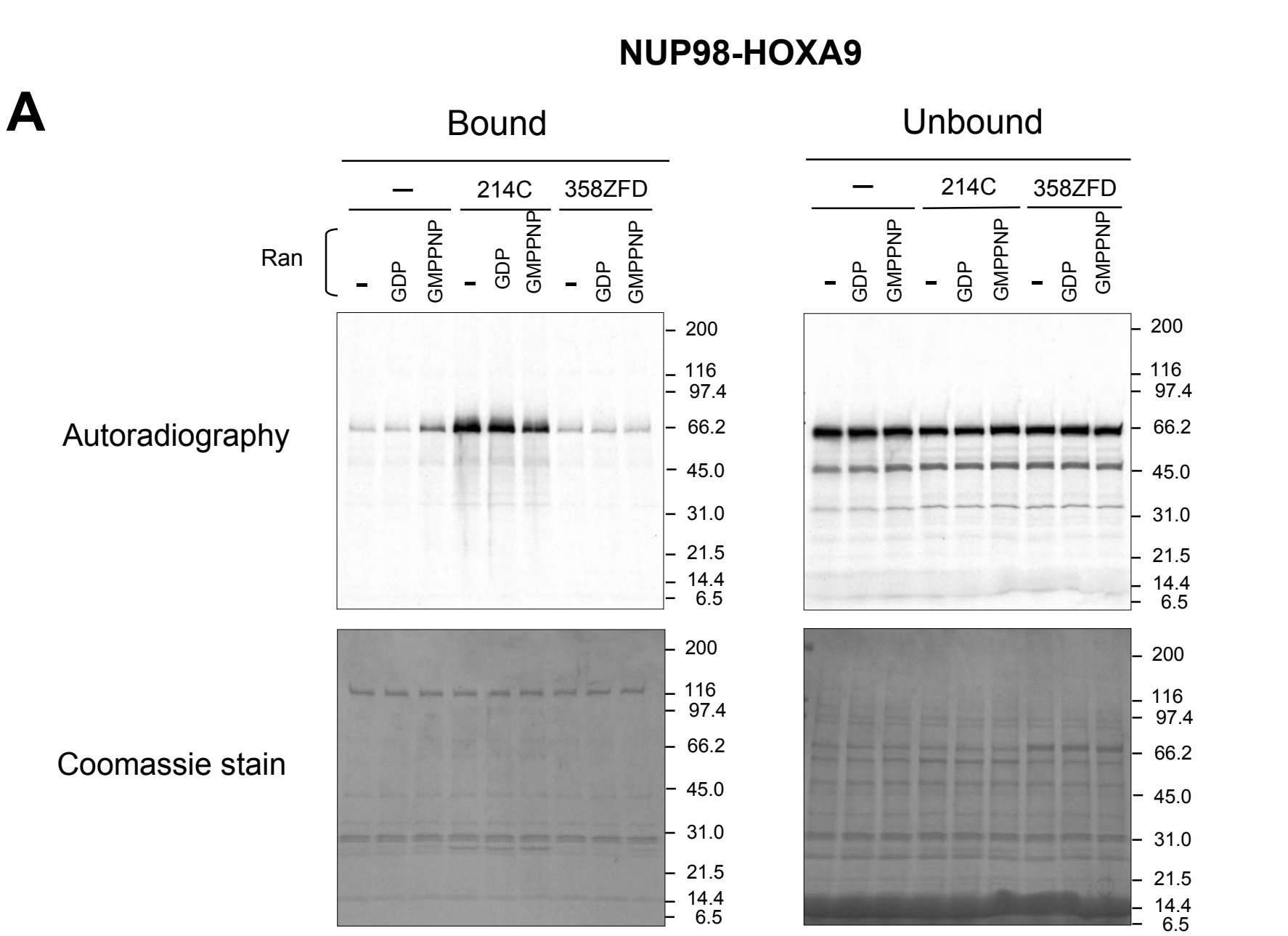

Supplementary Fig. 5A

NUP98-DDX10

B

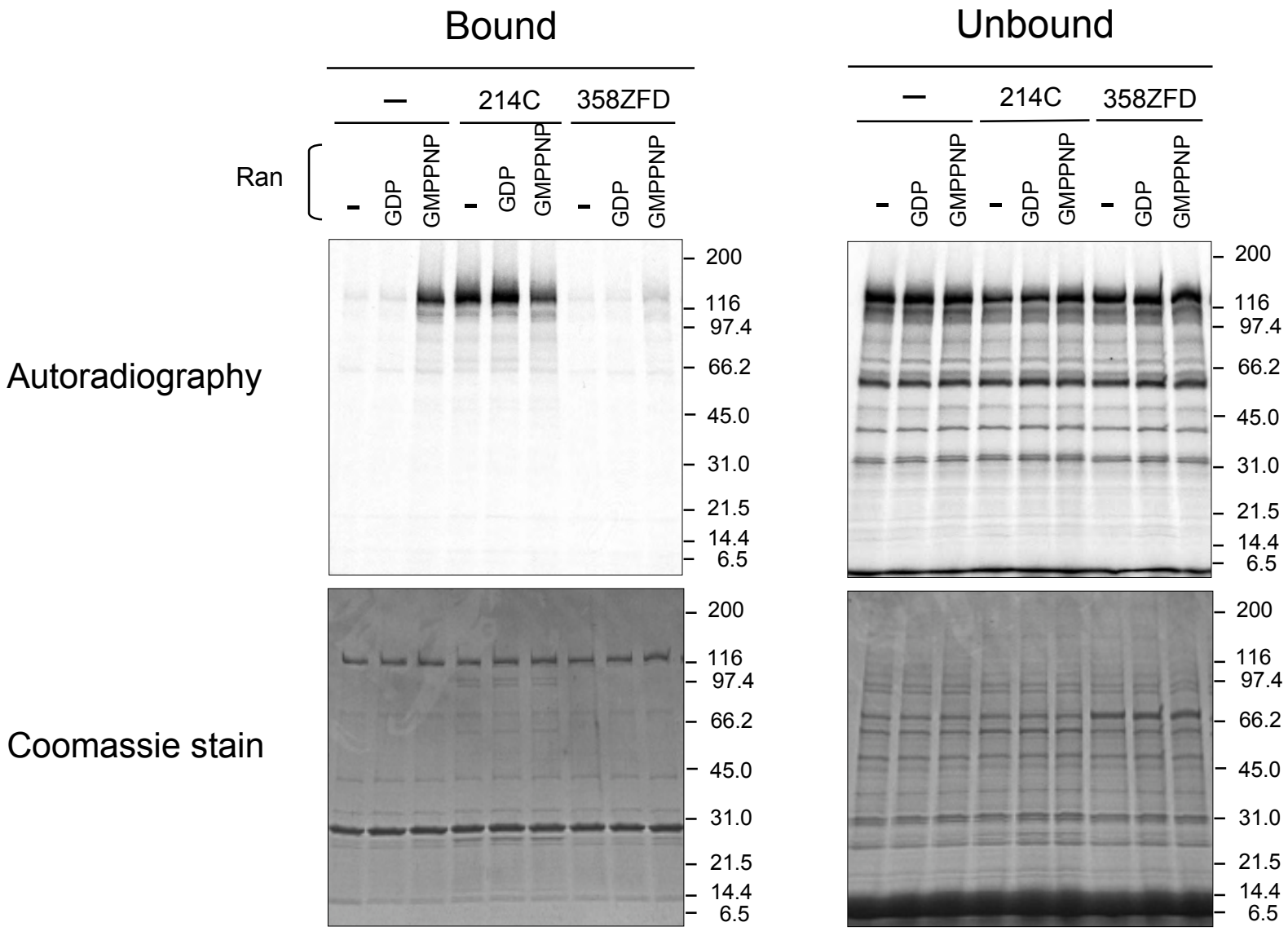

Supplementary Fig. 5B

NUP98

C

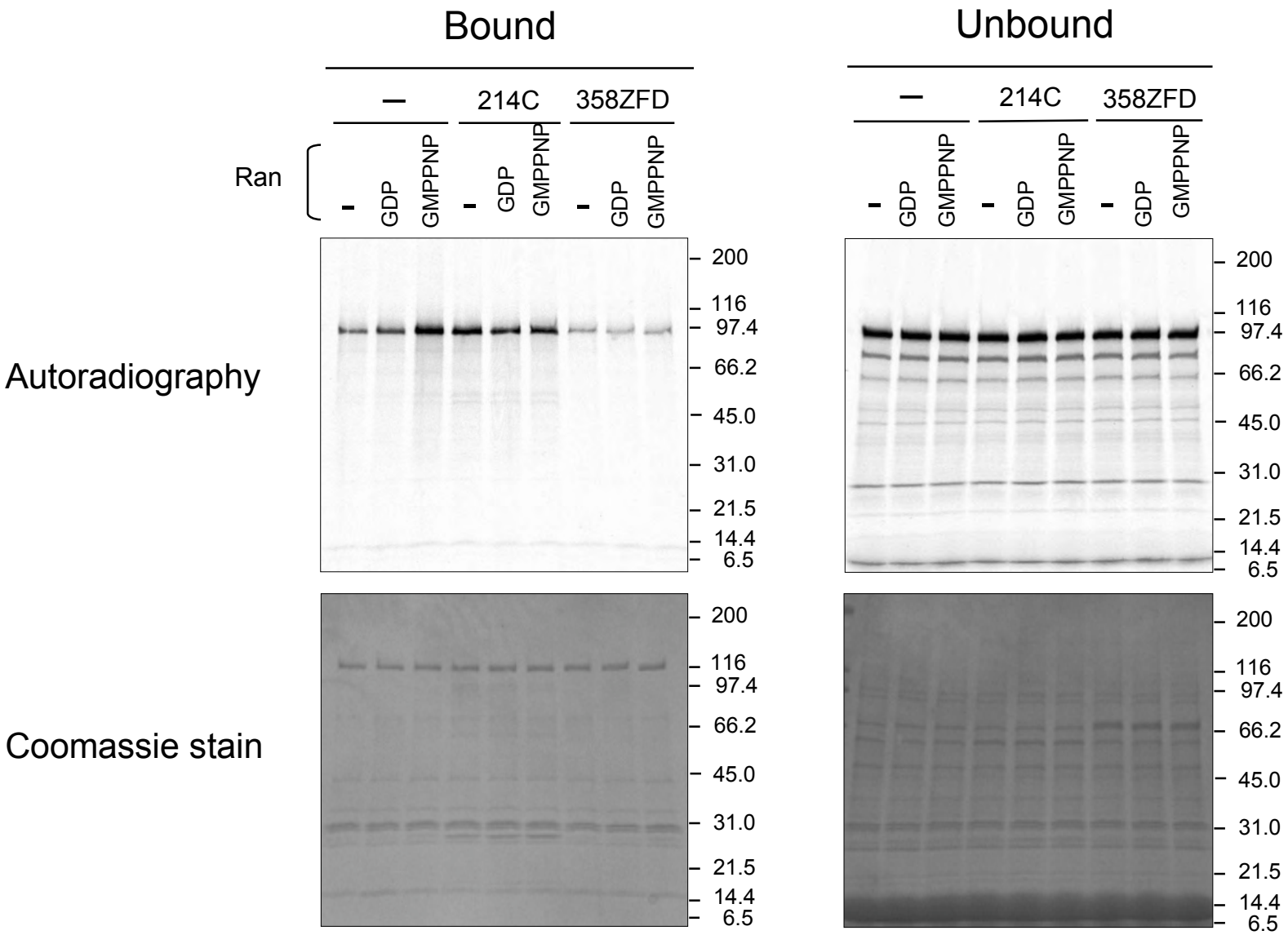

Supplementary Fig. 5C

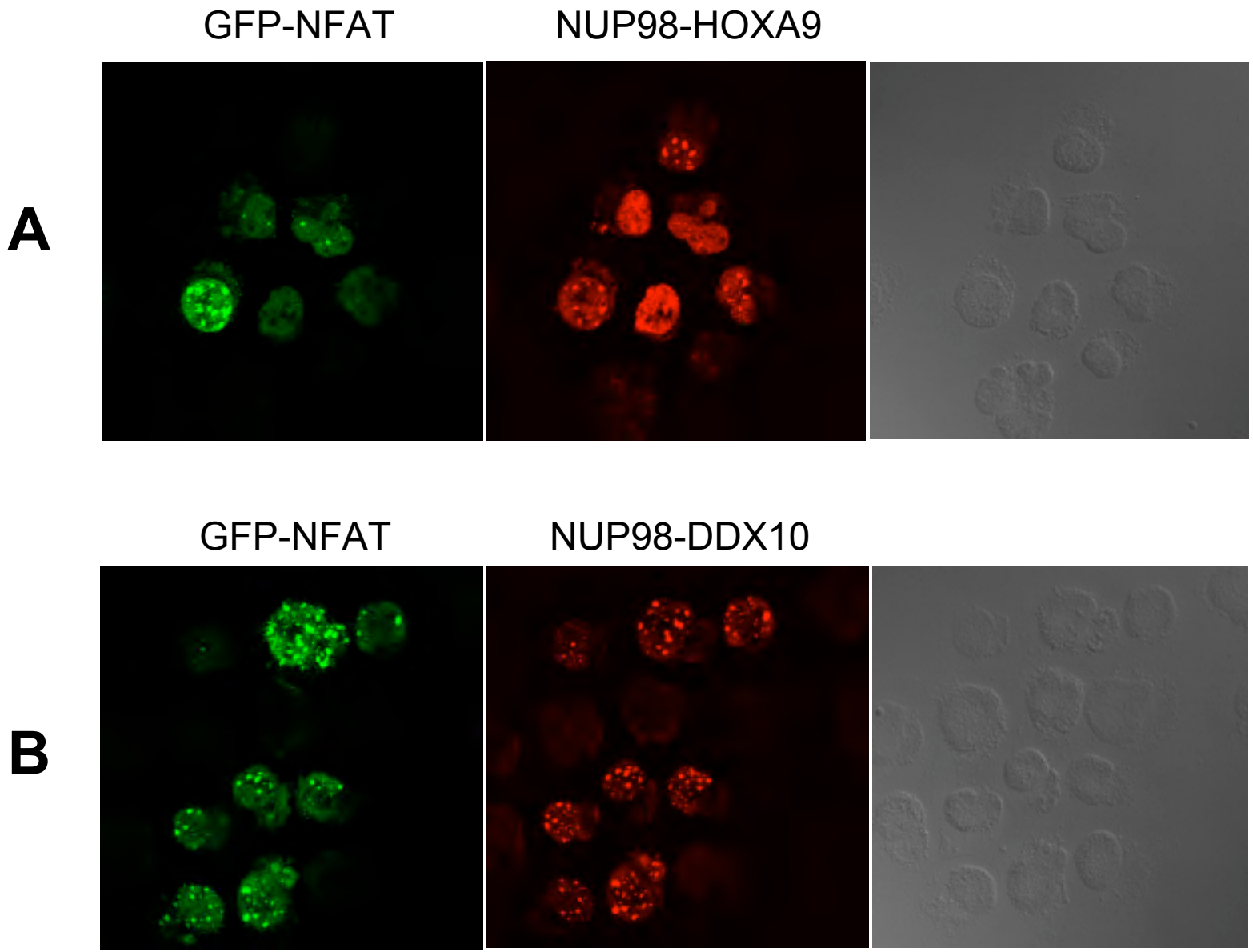

Supplementary Fig. 6AB

C

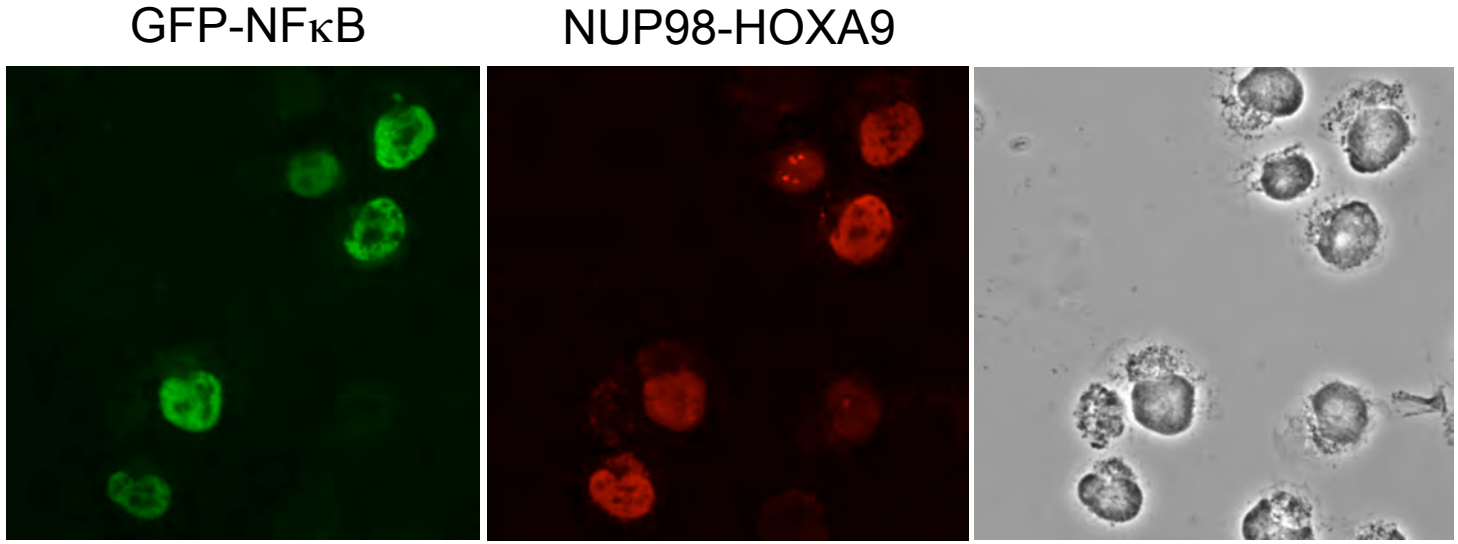

D

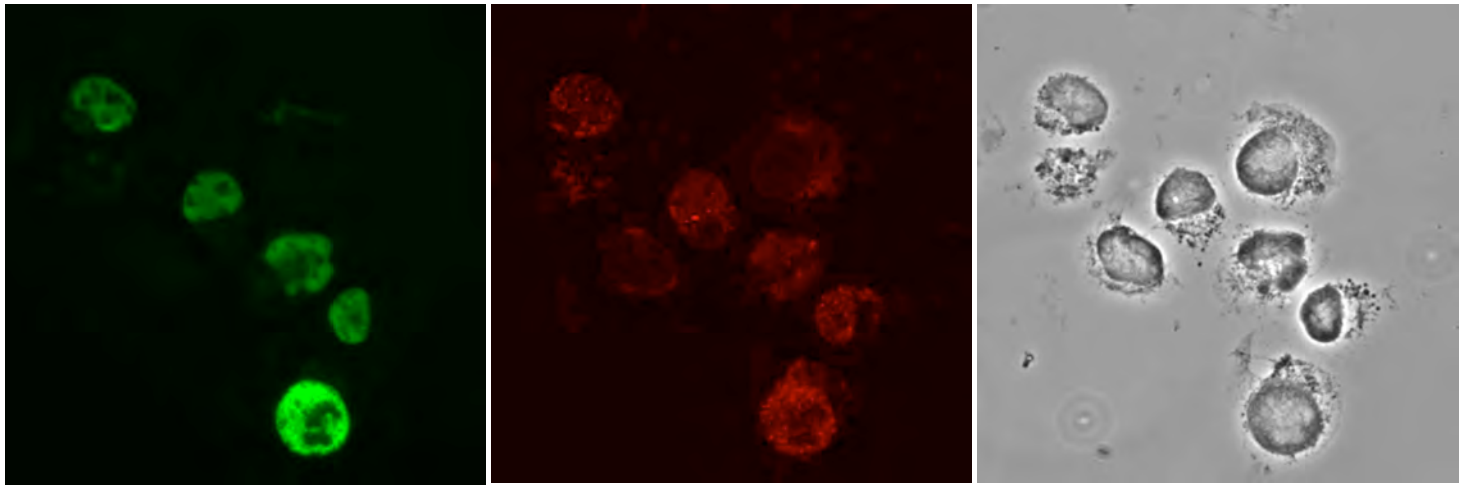

Supplementary Fig. 6CD

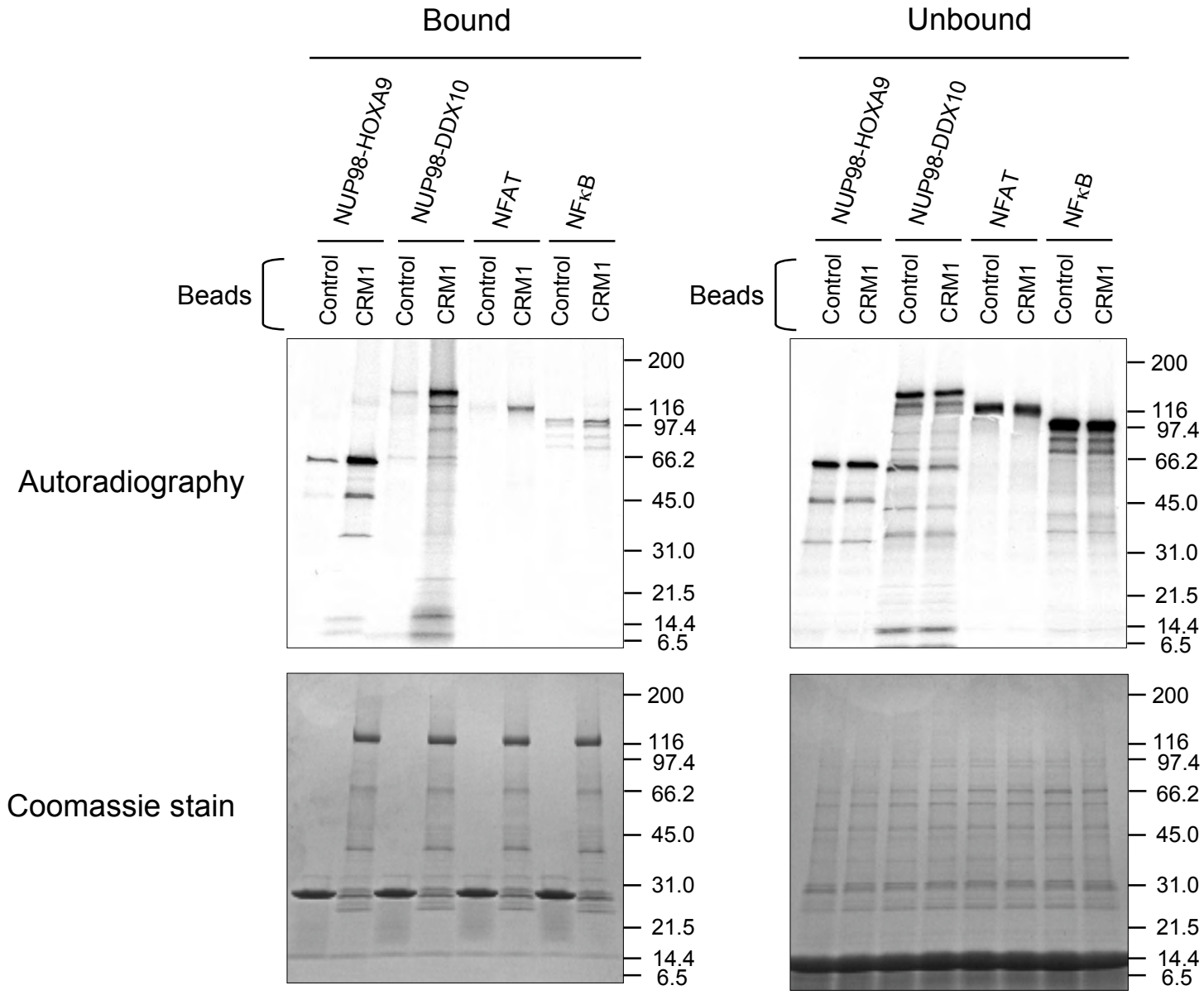

Supplementary Fig. 6E

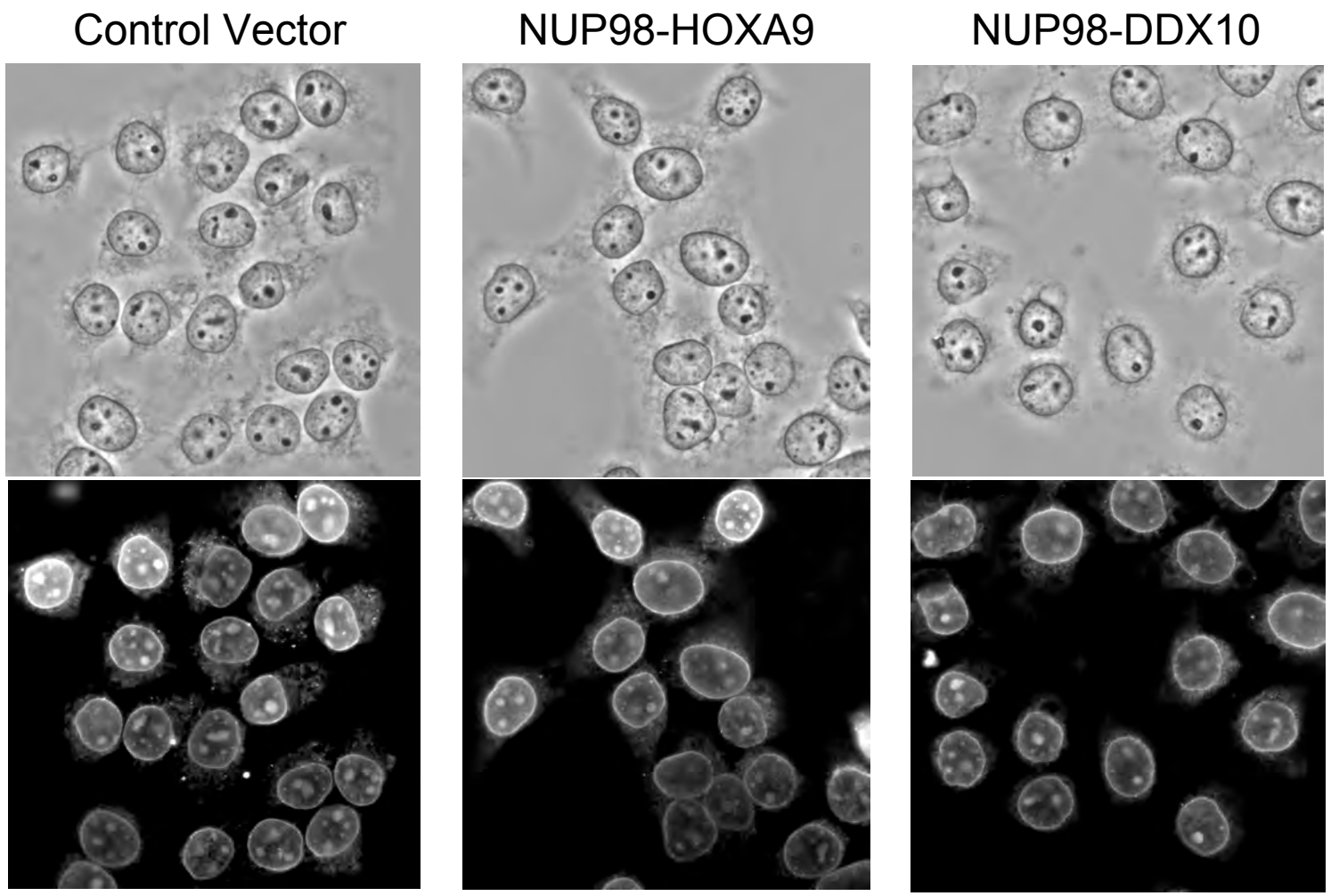

	Control Vector	NUP98-HOXA9	NUP98-DDX10
Average Intranuclear Fluorescence	214 ± 125	154 ± 66.2	177 ± 56.9

Supplementary Fig. 7

Supplementary Figure Legends

Supplementary Figure 1. **NUP98-HOXA9 is expressed in cells that show nuclear retention of CRM-1 export substrates.** K562 cells were nucleofected with EGFP-NPMc (*A*) or GFP-Rev (*B*) along with vector expressing NUP98-HOXA9. Cells were immunostained with anti-HA antibody in combination with Alexa Fluor 647-conjugated secondary antibody. The left panels show GFP images, the middle panels show anti-HA stains, and the right panels show corresponding phase contrast images. Images were viewed using a Nikon Eclipse 80i microscope with a Nikon 40X, 0.75 numerical aperture CFI Plan Fluor DLL objective and were acquired with a Nikon Coolsnap ES camera using MetaMorph 6.3r2 software.

Supplementary Figure 2. **NUP98-HOXA9 binds CRM1 through the FG motif in a Ran-GTP-dependent manner.** ^{35}S-labeled NUP98-HOXA9 and its variants were incubated with GST (Control) or GST-CRM1 (CRM1) immobilized on glutathione Sepharose 4B beads in the presence or absence of RanGDP or the RanGTP analog, RanGMPPNP. Uncropped autoradiographs and Coomassie-stained gels of bound and unbound fractions of reactions containing NUP98-HOXA9 (*A*), NUP98-HOXA9ΔN (*B*), NUP98-HOXA9ΔM (*C*), NUP98-HOXA9ΔJ (*D*), NUP98-HOXA9ΔNUP (*E*), and NUP98 (*F*) are shown. The positions of molecular mass markers (expressed in kilodaltons) are shown. Corresponding cropped autoradiographs are shown in Figure 2*B*.

Supplementary Figure 3. **NUP98-HOXA9 binding to CRM1 is stronger than that of CRM1export substrates.** ^{35}S-labeled NUP98-HOXA9, NUP98, NPMc, and Rev were incubated with GST-CRM1 immobilized on glutathione Sepharose 4B beads in the presence of RanGMPPNP with or without the indicated amount of Leptomycin B (LMB). Uncropped autoradiographs and Coomassie-stained gels are shown. The positions of molecular mass markers (expressed in kilodaltons) are shown. Corresponding cropped autoradiographs are shown in Figure 2*D*.

Supplementary Figure 4. **Rev binds specifically to CRM1.** ^{35}S-labeled Rev was incubated with GST (Control) or GST-CRM1 (CRM1) immobilized on glutathione Sepharose 4B beads in the presence of RanGMPPNP with or without 2 μM Leptomycin B (LMB). Approximately 30% of the total bound material and 10% of total unbound material for each reaction were analyzed as shown. Autoradiographs and Coomassie-stained gels are shown. The positions of molecular mass markers (expressed in kilodaltons) are shown.

Supplementary Figure 5. **NUP98 fusion proteins and NUP98 interact differently with NUP214.** ^{35}S-labeled NUP98-HOXA9, NUP98-DDX10, and NUP98 were incubated with GST-CRM1 immobilized on glutathione Sepharose 4B beads in the presence or absence of RanGDP or RanGMPPNP, with or without NUP214C or NUP358ZFD proteins as indicated. Uncropped autoradiographs and Coomassie-stained gels of bound and unbound fractions of reactions containing NUP98-HOXA9 (*A*), NUP98-DDX10 (*B*), and NUP98 (*C*) are shown. The positions of molecular mass markers (expressed in kilodaltons) are shown. Corresponding cropped autoradiographs are shown in Figure 4.

Supplementary Figure 6. **NUP98 fusions are expressed in cells that show nuclear retention of NFAT and NFκB.** K562 cells were nucleofected with GFP-NFAT (*A* and *C*) or EGFP-NFκB(p65) (*B* and *D*) along with vector expressing NUP98-HOXA9 (*A* and *B*) or NUP98-DDX10 (*C* and *D*). Cells were immunostained with anti-HA antibody in combination with Alexa Fluor 647-conjugated secondary antibody. The left panels show GFP images, the middle panels show anti-HA stains, and the right panels show corresponding DIC or phase contrast images. The images in *A* and *B* were acquired with a Zeiss LSM510 Meta laser scanning confocal microscope equipped with a Zeiss 63X, 1.4 numerical aperture Plan Apochromat oil objective using Zeiss LSM510 software. Images in *C* and *D* were viewed using a

Nikon Eclipse 80i microscope with a Nikon 40X, 0.75 numerical aperture CFI Plan Fluor DLL objective and were acquired with a Nikon Coolsnap ES camera using MetaMorph 6.3r2 software.

Supplementary Figure 7. **NUP98 fusions do not enhance nuclear import.** HeLa cells were retrovirally transduced with control vector or vector expressing NUP98-HOXA9 or NUP98-DDX10 and grown on cover slips. Cells were permeabilized with 35 μg/ml digitonin in transport buffer (20 mM HEPES-KOH, pH 7.3, 110 mM potassium acetate and 2 mM magnesium acetate). Import assays were carried out essentially as described (1,2) using a fluorescent import substrate (TRITC-BSA; 0.4 μg/ml) in the presence of RanGDP (0.6 μg/ml), karyopherin α1 (1 μg/ml) and β1 (0.5 μg/ml), and an energy-regenerating system. The lower panels show fluorescent images and the upper panels show corresponding phase contrast images. Images were viewed using a Nikon Eclipse 80i microscope with a Nikon 40X, 0.75 numerical aperture CFI Plan Fluor DLL objective and were acquired with a Nikon Coolsnap ES camera using MetaMorph 6.3r2 software. The intranuclear fluorescence intensity of 100 cells from each sample was measured using MetaMorph 6.3r2 software; the average intranuclear fluorescence intensity and standard deviation are shown.

1. Moore, M. S., and Blobel, G. (1992) *Cell* **69**, 939-950
2. Zhong, H., Takeda, A., Nazari, R., Shio, H., Blobel, G., and Yaseen, N. R. (2005) *J. Biol. Chem.* **280**, 10675-10682